Published in final edited form as:

J Am Soc Mass Spectrom. 2023 June 07; 34(6): 986–990. doi:10.1021/jasms.3c00005.

Interspecies Variation Affects IAPP Membrane Binding

Henry M. Sanders[1], **Farzaneh Chalyavi**[2], **Caitlyn R. Fields**[2], **Marius M. Kostelic**[1], **Ming-Hao Li**[3], **Daniel P. Raleigh**[3], **Martin T. Zanni**[2], **Michael T. Marty**[1,*]

[1]Department of Chemistry and Biochemistry and Bio5 Institute, University of Arizona, Tucson, AZ 85721, USA

[2]Department of Chemistry, University of Wisconsin-Madison, Madison, WI 53706, USA

[3]Department of Chemistry and Laufer Center for Quantitative Biology, Stony Brook University, 100 Nicolls Rd., Stony Brook, New York 11794, USA

Abstract

The aggregation of islet amyloid polypeptide (IAPP) is associated with β-cell dysfunction in type 2 diabetes (T2D) in humans. One possible mechanism of toxicity is the interaction of IAPP oligomers with lipid membranes to disrupt bilayer integrity and/or homeostasis of the cell. Amino acid sequence variations of IAPP between species can greatly decrease their propensity for aggregation. For example, human IAPP is toxic to β-cells, but rat and pig IAPP are not. However, it is not clear how these differences affect membrane association Using native mass spectrometry with lipid nanodiscs, we explored the differences in the association of human, rat, and pig IAPP with lipid bilayers. We discovered that human and rat IAPP bound nanodiscs with anionic dipalmitoyl-phosphatidylglycerol (DPPG) lipids, but pig IAPP did not. Furthermore, human and rat IAPP interacted differently with the membrane. Human IAPP show potential tetramer complexes, but rat IAPP associated with the membrane sequentially. Thus, overall IAPP-bilayer interactions are not necessarily related to disease, but small differences in oligomeric behaviour at the membrane may instead play a role.

Graphical Abstract

*Corresponding Author mtmarty@arizona.edu.

ASSOCIATED CONTENT

Supporting Information.

Supplemental methods, predicted mass defect tables, peptide sequences, and supporting native mass spectra including raw spectra and rIAPP and pIAPP at different concentrations. This material is available free of charge via the Internet at http://pubs.acs.org.

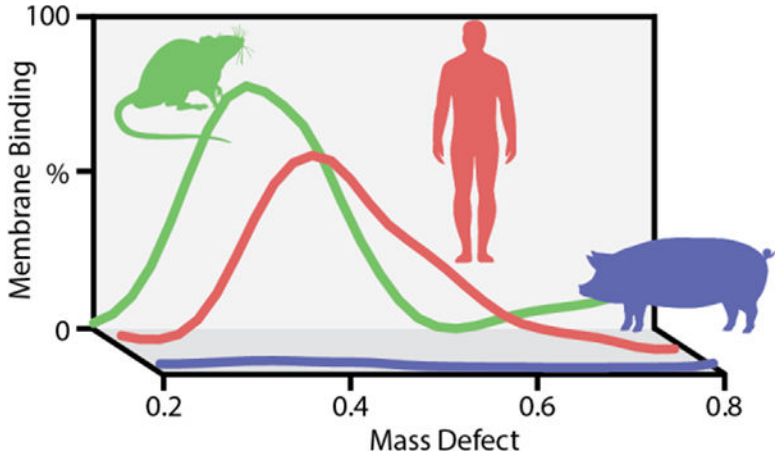

Introduction

The aggregation of the islet amyloid polypeptide (IAPP, also known as amylin) and deposition of fibrillar plaques in the pancreas is a pathological characteristic in type 2 diabetes (T2D).[1,2] IAPP is secreted from pancreatic cells alongside insulin and can aggregate through non-native β-sheet intermolecular interactions.[3,4] As with many misfolding proteins, it is difficult to characterize oligomeric intermediates that are present prior to fibrillization.

Interestingly, differences in the sequence of IAPP between species alters the propensity for aggregation and toxicity.[5,6] For example, human IAPP aggregates following excessive caloric intake.[5] In contrast, rats and pigs have more robust IAPP variants that do not aggregate, and these species are also less prone to T2D.[1,7] When transgenic rats with human IAPP are exposed to high fat diets, they develop T2D, which suggests a role for IAPP in pathogenesis.[8–10]

Misfolded protein aggregates are often associated with neurodegenerative diseases. Like other amyloidogenic proteins, the toxicity of IAPP is thought to be linked to transient oligomeric species, rather than fibrillar aggregates.[11,12] However, little is known about the structure of these IAPP oligomers. Molecular dynamics studies suggest that both aggregating and non-aggregating variants of IAPP form helical structures that may play functional roles, but the oligomerisation of IAPP depends on the non-native β-sheet structure.[13,14] Using 2D IR spectroscopy, Zanni and co-workers have observed an intermediate with beta-sheet-like structure in the central region of IAPP, a segment of the polypeptide that correlates with aggregation and disease.[13–15]

Interactions of oligomers with lipid membranes may also be important to disease mechanisms. IAPP can form pore-like structures in the membrane that are capable of transmitting ions in a potentially toxic manner.[3,16,17] However, IAPP has also been shown to have detergent-like effects on the membrane, eventually leading to membrane disruption.[11,18,19] Currently, it is unclear the degree to which unregulated ion transmission, detergent-like solubilisation, or both are responsible for cellular toxicity.[16,20] It is also

unclear how many oligomers constitute these membrane-bound species. Furthermore, there are reports that the growth of amyloid fibrils on membranes is responsible for hIAPP-induced membrane disruption.[21,22] Miranker and co-workers detected oligomers by crosslinking that were as high as hexamers in the presence of DOPG liposomes. These higher order oligomers were correlated with membrane leakage and an increase in the rate of fibril formation.[23]

Here, we use native mass spectrometry (MS) to investigate how different IAPP variants from human, rat (rIAPP) and pig (pIAPP) associated differently with membranes in lipid nanodiscs. hIAPP is linked to T2D, but rIAPP and pIAPP are not.[5] Our goal was to test how these different sequences affect membrane binding and if there were trends that correlated with their disease relevance. We chose rat and porcine variants of IAPP because they are not amyloid-forming and are nontoxic in normal physiological conditions.[3,8,24] Sequences of the three polypeptides are shown in Figure S1. Relative to hIAPP, rIAPP includes three Pro substitutions and an H18R substitution, along with two more conservative changes. The porcine peptide differs from hIAPP at 10 positions, and five of these are within the 20–29 region thought to be critical for amyloid formation.

The oligomerization and structure of IAPP in solution have been studied by native MS previously, typically in tandem with ion mobility (IMMS).[25–27] Bowers and co-workers discovered that monomeric β-hairpin structures were only present in hIAPP and not rIAPP, suggesting a self-associating structural motif.[25] This structural population increased at pH 8.0, which correlated with increased fibrillation. Later work revealed that dimeric hIAPP also contained β-rich structure, which was absent in rIAPP dimers.[26] Radford, Ashcroft, and co-workers used native IMMS to screen small molecule-hIAPP complexes and study their mode of inhibition. They discovered a new hIAPP inhibitor and highlighted the versatility of native MS for studying structures and interactions of IAPPs in solution.[27]

Here, we used lipid nanodiscs as membrane mimetics to measure IAPP interactions in a controlled model membrane environment. Nanodiscs provide the unique ability to monitor stoichiometric binding to the bilayer with native MS. We assembled nanodiscs as previously described[28–30] with either zwitterionic 1,2-dipalmitoyl-*sn*-glycero-3-phosphocholine (DPPC) or anionic 1,2-dipalmitoyl-*sn*-glycero-3-phospho-(1'-rac-glycerol) (DPPG) to modulate the nanodisc surface charges. Full experimental methods can be found in Supplemental Information.

hIAPP, rIAPP, and pIAPP were synthesized via solid-phase peptide synthesis[15,31] Aliquots were diluted to desired concentration in 200 mM ammonium acetate at three stock concentrations. 3 μL of each IAPP stock were added to 19 μL of nanodiscs (2.2 μM final concentration) for final IAPP concentrations of 6.8, 20.5, and 40.9 μM. This equates to roughly 3:1, 9:1, and 18:1 IAPP:nanodisc ratios, respectively. Samples were incubated while being gently rocked at room temperature for 1 hour.

Native mass spectra of the intact nanodisc complexes with associated peptides were collected using a Q-Exactive HF UHMR mass spectrometer (Thermo Fisher Scientific, Bremen, Germany). Nanodiscs naturally have a roughly Gaussian distribution in mass

caused by the variation in total lipids per complex. Additionally, nanodiscs will acquire several different charge states for a complex *m/z* spectrum (Figure S2). Thus, we first used UniDec to deconvolve the *m/z* spectrum into a zero-charge mass spectrum (Figure 1A). The mass distributions were then analyzed using macromolecular mass defect analysis (Figure 1B).[28,30] Macromolecular mass defect analysis gives stoichiometric information of non-lipid masses, e.g. IAPP, that are bound to nanodiscs. We have previously used this technique for analysis of interactions between α-synuclein and antimicrobial peptides, and nanodiscs.[28–30,32] The reference masses used for mass defect analysis for each IAPP variant are listed in Tables S1 and S2.

hIAPP Forms Tetramers with Anionic Membranes

We first explored hIAPP–membrane interactions with nanodiscs with different head groups. All IAPP variants carry a net positive charge at neutral pH, and hIAPP is known to interact with anionic membranes.[33,34] Thus, we compared hIAPP interactions in zwitterionic DPPC nanodiscs with anionic DPPG nanodiscs.

We did not detect any hIAPP associating with zwitterionic DPPC nanodiscs (Figure S3). In contrast, hIAPP easily associated with DPPG nanodiscs at hIAPP:nanodisc ratios of 9:1 and 18:1. This association was evidenced by a concentration dependent increase in the mass defect peaks for hIAPP–nanodisc complexes (Figure 1B). Thus, hIAPP has a higher affinity for the anionic DPPG nanodiscs.

Although hIAPP has been shown to interact with zwitterionic membranes,[14,34] bilayers with a higher anionic content show more pronounced effects on IAPP behaviour, such as a greater aggregation propensity or bilayer leakage.[34] Electrostatic attraction to anionic membranes is a driving force of other peptide-membrane interactions, particularly amyloid-β and α-synuclein.[28,35–37]

At 18:1 hIAPP:nanodisc, macromolecular mass defect analysis revealed not only 1 bound hIAPP per nanodisc species but also signal for 4 bound hIAPP per nanodisc (Figure 1C). We attribute this stoichiometry of 4 bound hIAPP per nanodisc to the formation of tetrameric oligomers. If 4 monomers bound to the nanodisc without forming specific oligomer, then membrane association with multiple peptides should increase sequentially with concentration, forming a roughly Poisson distributions, as previously observed.[28–30] Here, the absence of bound hIAPP with 2, 3, and higher stoichiometries per nanodisc is inconsistent with a Poisson distribution of bound monomers, so we conclude that a tetrameric oligomer is associated with the nanodisc. Native MS in the absence of nanodiscs showed no oligomer formation (Figure S4). Others have seen oligomer formation by MS, but our IAPP concentrations were typically lower and incubated for only an hour.[38] The lack of oligomeric species may also be due to optimization of the instrument toward higher mass species, making small and low abundance oligomers difficult to detect.

Interestingly, the overall nanodisc assembly with an associate tetramer has a lower mass compared nanodisc assemblies with only the monomer. This decrease could suggest the tetramer is inserting into the bilayer with lipids being displaced to accommodate it, rather than sitting atop the surface and adding mass, like the monomer (Figure 1C). Alternatively, it

could also suggest a bias towards association with less tightly packed nanodiscs. In any case, the lower abundance of tetramers over monomers is likely because pre-fibrillar intermediates are typically detected in only small amounts.[13,34]

Oligomeric structures of hIAPP have previously been shown to form channels with widths capable of accommodating water, Na^+, and Ca^{2+}, which could explain a mechanism of cellular toxicity through unregulated permeability.[11] Anionic lipids are known to stabilise such structures, as well as catalyse their formation.[14,16] Our work adds further evidence showing hIAPP can form specific oligomeric complexes in anionic bilayers.

IAPP from Different Species Associate with Nanodiscs Differently

After examining hIAPP-membrane association, we next investigated interactions of isoforms from pig and rat. rIAPP and pIAPP were incubated with DPPG nanodiscs at the same concentrations and conditions as hIAPP. Following incubation, spectra of the sample mixtures were collected, and mass defect were observed for each (Figure 2). Here, rIAPP had a greater propensity for association with DPPG nanodiscs than hIAPP (Figure 2A–D, S5). In contrast, pIAPP showed no signs of association with the membrane at any concentration (Figure 2E–F, S6). This lack of binding could be because pIAPP contains fewer overall cationic residues than hIAPP and rIAPP (Figure S1).

These results are particularly interesting because neither rIAPP nor pIAPP are disease associated. Thus, the differences in membrane association between these three species suggest there is no correlation between global membrane association and disease relevance. Although membrane association of hIAPP maybe be involved in a disease mechanism, non-amyloidogenic isoforms like rIAPP may still bind the membrane in a non-destructive manner. rIAPP and other IAPP variants have been shown to disrupt model anionic membranes at concentrations where they are not significantly toxic to cultured cells.[39] Similarly, we previously showed α-synuclein can bind nanodiscs without disruption, provided a fibril inhibitor was present.[28]

Interestingly, at 9:1 and 18:1 ratios of added IAPP:nanodisc, a small signal was present in the mass defect region for 2 bound rIAPP but not for higher stoichiometries (Figure 2D and Figure S5). More nanodiscs with 1 and 2 bound rIAPP were observed at the 18:1 ratio than 9:1. Ratios higher than 18:1 were attempted, but the spectra were unresolvable. The data for 2 bound rIAPP differed from the tetramer observed in hIAPP in two critical ways. First, the sequential addition of rIAPP to the nanodisc, i.e. 1 and 2 bound rIAPP, differed from hIAPP, which had a non-sequential mixture of 1 and 4 bound hIAPP at the highest concentration tested (Figure 1C). Moreover, the mass of the nanodiscs assembly with 2 bound rIAPP is higher than the nanodisc assembly with 1 bound rIAPP, unlike hIAPP where the 4 bound assembly is lower in mass. These two factors indicate that rIAPP is likely not forming dimers but rather that two rIAPP are binding the membrane randomly due to the increased statistical probability of bilayer association as the rIAPP concentration increases. Despite this, it is possible a dimer of rIAPP could be binding the membrane as shown in previously.[40] rIAPP contains three proline substitutions along with F23L and H18R substitutions that may disrupt the formation of β-sheet structure, which is thought to

be necessary for aggregation. These resides may also be important to the stabilisation of higher order structures, like tetramers.[13,14,41,42]

Overall, we found that hIAPP membrane association is charge dependent and that hIAPP forms tetramer complexes in DPPG membranes at micromolar concentrations. In contrast, non-amyloidogenic rIAPP bound DPPG membranes with high affinities but did not show tetramer formation. Non-amyloidogenic pIAPP showed no detectable membrane association. Together, these data suggest that differences in the affinity of IAPP for anionic membrane are species specific but not correlated with disease. These new insights broaden our understanding of how IAPP interacts with membranes between species and how this interaction relates to disease.

Supplementary Material

Refer to Web version on PubMed Central for supplementary material.

ACKNOWLEDGMENT

The authors thank Alexander Makarov, Maria Reinhardt-Szyba, and Kyle Fort at Thermo Fisher Scientific for support on the UHMR Q-Exactive HF instrument. The pMSP1D1 plasmid was a gift from Stephen Sligar (Addgene plasmid 20061).

Funding Sources

Funding was provided by the National Institutes of Health/National Institute of General Medical Sciences (NIH/NIGMS) under R35 GM128624 to M.T.M. and from the National Institutes of Health R01DK079895 to M.T.Z and from the National Institutes of Health GM078114 to D.P.R.

REFERENCES

(1). Asthana S; Mallick B; Alexandrescu AT; Jha S IAPP in Type II Diabetes: Basic Research on Structure, Molecular Interactions, and Disease Mechanisms Suggests Potential Intervention Strategies. Biochim. Biophys. Acta - Biomembr. 2018, 1860 (9), 1765–1782. 10.1016/j.bbamem.2018.02.020. [PubMed: 29518374]

(2). Dobson CM Principles of Protein Folding, Misfolding and Aggregation. Semin. Cell Dev. Biol. 2004, 15 (1), 3–16. 10.1016/j.semcdb.2003.12.008. [PubMed: 15036202]

(3). Cao P; Abedini A; Raleigh DP Aggregation of Islet Amyloid Polypeptide: From Physical Chemistry to Cell Biology. Curr. Opin. Struct. Biol. 2013, 23 (1), 82–89. 10.1016/j.sbi.2012.11.003. [PubMed: 23266002]

(4). Sun Y; Wang B; Ge X; Ding F Distinct Oligomerization and Fibrillization Dynamics of Amyloid Core Sequences of Amyloid-Beta and Islet Amyloid Polypeptide. Phys. Chem. Chem. Phys. 2017, 19 (41), 28414–28423. 10.1039/C7CP05695H. [PubMed: 29038815]

(5). Wu C; Shea J-E Structural Similarities and Differences between Amyloidogenic and Non-Amyloidogenic Islet Amyloid Polypeptide (IAPP) Sequences and Implications for the Dual Physiological and Pathological Activities of These Peptides. PLoS Comput. Biol. 2013, 9 (8), e1003211. 10.1371/journal.pcbi.1003211. [PubMed: 24009497]

(6). Jotha-Mattos L; Vieira AB; Castelo M. da S. M.; Queiroz A. S. de M.; de Souza HJM; de Alencar NX; Lima LMTR Amyloidogenesis of Feline Amylin and Plasma Levels in Cats with Diabetes Mellitus or Pancreatitis. Domest. Anim. Endocrinol. 2021, 74, 106532. 10.1016/j.domaniend.2020.106532. [PubMed: 32841886]

(7). Betsholtz C; Svensson V; Rorsman F; Engström U; Westermark GT; Wilander E; Johnson K; Westermark P Islet Amyloid Polypeptide (IAPP): CDNA Cloning and Identification of an Amyloidogenic Region Associated with the Species-Specific Occurrence of Age-Related

Diabetes Mellitus. Exp. Cell Res. 1989, 183 (2), 484–493. 10.1016/0014-4827(89)90407-2. [PubMed: 2670595]

(8). Höppener JWM; Jansz HS; Oosterwijk C; van Hulst KL; Lips CJM; Verbeek JS; Capel PJA; de Koning EJP; Clark A Molecular Physiology of the Islet Amyloid Polypeptide (IAPP)/Amylin Gene in Man, Rat, and Transgenic Mice. J. Cell. Biochem. 1994, 55 (S1994A), 39–53. 10.1002/jcb.240550006. [PubMed: 7929617]

(9). Verchere CB; D'Alessio DA; Palmiter RD; Weir GC; Bonner-Weir S; Baskin DG; Kahn SE Islet Amyloid Formation Associated with Hyperglycemia in Transgenic Mice with Pancreatic Beta Cell Expression of Human Islet Amyloid Polypeptide. Proc. Natl. Acad. Sci. 1996, 93 (8), 3492–3496. 10.1073/pnas.93.8.3492. [PubMed: 8622964]

(10). Hull RL; Andrikopoulos S; Verchere CB; Vidal J; Wang F; Cnop M; Prigeon RL; Kahn SE Increased Dietary Fat Promotes Islet Amyloid Formation and β-Cell Secretory Dysfunction in a Transgenic Mouse Model of Islet Amyloid. Diabetes 2003, 52 (2), 372–379. 10.2337/diabetes.52.2.372. [PubMed: 12540610]

(11). Brender JR; Salamekh S; Ramamoorthy A Membrane Disruption and Early Events in the Aggregation of the Diabetes Related Peptide IAPP from a Molecular Perspective. Acc. Chem. Res. 2012, 45 (3), 454–462. 10.1021/ar200189b. [PubMed: 21942864]

(12). Abedini A; Plesner A; Cao P; Ridgway Z; Zhang J; Tu L-H; Middleton CT; Chao B; Sartori DJ; Meng F; Want H; Wong AG; Zanni MT; Verchere CB; Raleigh DP; Schmidt AM Time-Resolved Studies Define the Nature of Toxic IAPP Intermediates, Providing Insight for Anti-Amyloidosis Therapeutics. Elife 2016, 5. 10.7554/eLife.12977.

(13). Serrano AL; Lomont JP; Tu L-H; Raleigh DP; Zanni MT A Free Energy Barrier Caused by the Refolding of an Oligomeric Intermediate Controls the Lag Time of Amyloid Formation by HIAPP. J. Am. Chem. Soc. 2017, 139 (46), 16748–16758. 10.1021/jacs.7b08830. [PubMed: 29072444]

(14). Dicke SS; Maj M; Fields CR; Zanni MT Metastable Intermediate during HIAPP Aggregation Catalyzed by Membranes as Detected with 2D IR Spectroscopy. RSC Chem. Biol. 2022, 3 (7), 931–940. 10.1039/D2CB00028H. [PubMed: 35866164]

(15). Buchanan LE; Dunkelberger EB; Tran HQ; Cheng P-N; Chiu C-C; Cao P; Raleigh DP; de Pablo JJ; Nowick JS; Zanni MT Mechanism of IAPP Amyloid Fibril Formation Involves an Intermediate with a Transient β-Sheet. Proc. Natl. Acad. Sci. 2013, 110 (48), 19285–19290. 10.1073/pnas.1314481110. [PubMed: 24218609]

(16). Poojari C; Xiao D; Batista VS; Strodel B Membrane Permeation Induced by Aggregates of Human Islet Amyloid Polypeptides. Biophys. J. 2013, 105 (10), 2323–2332. 10.1016/j.bpj.2013.09.045. [PubMed: 24268144]

(17). Khemtémourian L; Antoinette Killian J; Höppener JWM; Engel MFM Recent Insights in Islet Amyloid Polypeptide-Induced Membrane Disruption and Its Role in Beta-Cell Death in Type 2 Diabetes Mellitus. Exp. Diabetes Res 2008, 2008, 1–9. 10.1155/2008/421287.

(18). Evers F; Jeworrek C; Tiemeyer S; Weise K; Sellin D; Paulus M; Struth B; Tolan M; Winter R Elucidating the Mechanism of Lipid Membrane-Induced IAPP Fibrillogenesis and Its Inhibition by the Red Wine Compound Resveratrol: A Synchrotron X-Ray Reflectivity Study. J. Am. Chem. Soc. 2009, 131 (27), 9516–9521. 10.1021/ja8097417. [PubMed: 19583433]

(19). Pithadia A; Brender JR; Fierke CA; Ramamoorthy A Inhibition of IAPP Aggregation and Toxicity by Natural Products and Derivatives. J. Diabetes Res. 2016, 2016, 1–12. 10.1155/2016/2046327.

(20). Fusco G; Chen SW; Williamson PTF; Cascella R; Perni M; Jarvis JA; Cecchi C; Vendruscolo M; Chiti F; Cremades N; Ying L; Dobson CM; De Simon A Structural Basis of Membrane Disruption and Cellular Toxicity by α-Synuclein Oligomers. Science 2017, 358 (6369), 1440–1443. 10.1126/science.aan6160. [PubMed: 29242346]

(21). Sparr E; Engel MFM; Sakharov DV; Sprong M; Jacobs J; de Kruijff B; Höppener JWM; Antoinette Killian J Islet Amyloid Polypeptide-Induced Membrane Leakage Involves Uptake of Lipids by Forming Amyloid Fibers. FEBS Lett. 2004, 577 (1–2), 117–120. 10.1016/j.febslet.2004.09.075. [PubMed: 15527771]

(22). Elenbaas BOW; Khemtemourian L; Killian JA; Sinnige T Membrane-Catalyzed Aggregation of Islet Amyloid Polypeptide Is Dominated by Secondary Nucleation. Biochemistry 2022, 61 (14), 1465–1472. 10.1021/acs.biochem.2c00184. [PubMed: 35749314]

(23). Knight JD; Hebda JA; Miranker AD Conserved and Cooperative Assembly of Membrane-Bound α-Helical States of Islet Amyloid Polypeptide. Biochemistry 2006, 45 (31), 9496–9508. 10.1021/bi060579z. [PubMed: 16878984]

(24). Potter KJ; Abedini A; Marek P; Klimek AM; Butterworth S; Driscoll M; Baker R; Nilsson MR; Warnock GL; Oberholzer J; Bertera S; Trucco M; Korbutt GS; Fraser PE; Raleigh DP; Verchere CB Islet Amyloid Deposition Limits the Viability of Human Islet Grafts but Not Porcine Islet Grafts. Proc. Natl. Acad. Sci. 2010, 107 (9), 4305–4310. 10.1073/pnas.0909024107. [PubMed: 20160085]

(25). Dupuis NF; Wu C; Shea J-E; Bowers MT Human Islet Amyloid Polypeptide Monomers Form Ordered β-Hairpins: A Possible Direct Amyloidogenic Precursor. J. Am. Chem. Soc. 2009, 131 (51), 18283–18292. 10.1021/ja903814q. [PubMed: 19950949]

(26). Dupuis NF; Wu C; Shea J-E; Bowers MT The Amyloid Formation Mechanism in Human IAPP: Dimers Have β-Strand Monomer–Monomer Interfaces. J. Am. Chem. Soc. 2011, 133 (19), 7240–7243. 10.1021/ja1081537. [PubMed: 21517093]

(27). Young LM; Saunders JC; Mahood RA; Revill CH; Foster RJ; Tu L-H; Raleigh DP; Radford SE; Ashcroft AE Screening and Classifying Small-Molecule Inhibitors of Amyloid Formation Using Ion Mobility Spectrometry–Mass Spectrometry. Nat. Chem. 2015, 7 (1), 73–81. 10.1038/nchem.2129. [PubMed: 25515893]

(28). Sanders HM; Kostelic MM; Zak CK; Marty MT Lipids and EGCG Affect α-Synuclein Association and Disruption of Nanodiscs. Biochemistry 2022, 61 (11), 1014–1021. 10.1021/acs.biochem.2c00160. [PubMed: 35616927]

(29). Walker LR; Marzluff EM; Townsend JA; Resager WC; Marty MT Native Mass Spectrometry of Antimicrobial Peptides in Lipid Nanodiscs Elucidates Complex Assembly. Anal. Chem. 2019, 91 (14), 9284–9291. 10.1021/acs.analchem.9b02261. [PubMed: 31251560]

(30). Walker LR; Marty MT Revealing the Specificity of a Range of Antimicrobial Peptides in Lipid Nanodiscs by Native Mass Spectrometry. Biochemistry 2020, 59 (23), 2135–2142. 10.1021/acs.biochem.0c00335. [PubMed: 32452672]

(31). Collins JM; Porter KA; Singh SK; Vanier GS High-Efficiency Solid Phase Peptide Synthesis (HE-SPPS). Org. Lett. 2014, 16 (3), 940–943. 10.1021/ol4036825. [PubMed: 24456219]

(32). Kostelic MM; Ryan AM; Reid DJ; Noun JM; Marty MT Expanding the Types of Lipids Amenable to Native Mass Spectrometry of Lipoprotein Complexes. J. Am. Soc. Mass Spectrom. 2019, 30 (8), 1416–1425. 10.1007/s13361-019-02174-x. [PubMed: 30972726]

(33). Saraogi I; Hebda JA; Becerril J; Estroff LA; Miranker AD; Hamilton AD Synthetic α-Helix Mimetics as Agonists and Antagonists of Islet Amyloid Polypeptide Aggregation. Angew. Chemie Int. Ed. 2010, 49 (4), 736–739. 10.1002/anie.200901694.

(34). Zhang X; St. Clair JR; London E; Raleigh DP Islet Amyloid Polypeptide Membrane Interactions: Effects of Membrane Composition. Biochemistry 2017, 56 (2), 376–390. 10.1021/acs.biochem.6b01016. [PubMed: 28054763]

(35). Sanders HM; Jovcevski B; Marty MT; Pukala TL Structural and Mechanistic Insights into Amyloid-β and A-synuclein Fibril Formation and Polyphenol Inhibitor Efficacy in Phospholipid Bilayers. FEBS J. 2022, 289 (1), 215–230. 10.1111/febs.16122. [PubMed: 34268903]

(36). Ghio S; Camilleri A; Caruana M; Ruf VC; Schmidt F; Leonov A; Ryazanov S; Griesinger C; Cauchi RJ; Kamp F; Giese A; Vassallo N Cardiolipin Promotes Pore-Forming Activity of Alpha-Synuclein Oligomers in Mitochondrial Membranes. ACS Chem. Neurosci. 2019, 10 (8), 3815–3829. 10.1021/acschemneuro.9b00320. [PubMed: 31356747]

(37). Musteikytė G; Jayaram AK; Xu CK; Vendruscolo M; Krainer G; Knowles TPJ Interactions of α-Synuclein Oligomers with Lipid Membranes. Biochim. Biophys. Acta - Biomembr. 2021, 1863 (4), 183536. 10.1016/j.bbamem.2020.183536. [PubMed: 33373595]

(38). Young LM; Tu L-H; Raleigh DP; Ashcroft AE; Radford SE Understanding Co-Polymerization in Amyloid Formation by Direct Observation of Mixed Oligomers. Chem. Sci. 2017, 8 (7), 5030–5040. 10.1039/C7SC00620A. [PubMed: 28970890]

(39). Cao P; Abedini A; Wang H; Tu L-H; Zhang X; Schmidt AM; Raleigh DP Islet Amyloid Polypeptide Toxicity and Membrane Interactions. Proc. Natl. Acad. Sci. 2013, 110 (48), 19279–19284. 10.1073/pnas.1305517110. [PubMed: 24218607]

(40). Nath A; Miranker AD; Rhoades E A Membrane-Bound Antiparallel Dimer of Rat Islet Amyloid Polypeptide. Angew. Chemie 2011, 123 (46), 11051–11054. 10.1002/ange.201102887.

(41). Jayasinghe SA; Langen R Lipid Membranes Modulate the Structure of Islet Amyloid Polypeptide. Biochemistry 2005, 44 (36), 12113–12119. 10.1021/bi050840w. [PubMed: 16142909]

(42). Ridgway Z; Eldrid C; Zhyvoloup A; Ben-Younis A; Noh D; Thalassinos K; Raleigh DP Analysis of Proline Substitutions Reveals the Plasticity and Sequence Sensitivity of Human IAPP Amyloidogenicity and Toxicity. Biochemistry 2020, 59 (6), 742–754. 10.1021/acs.biochem.9b01109. [PubMed: 31922743]

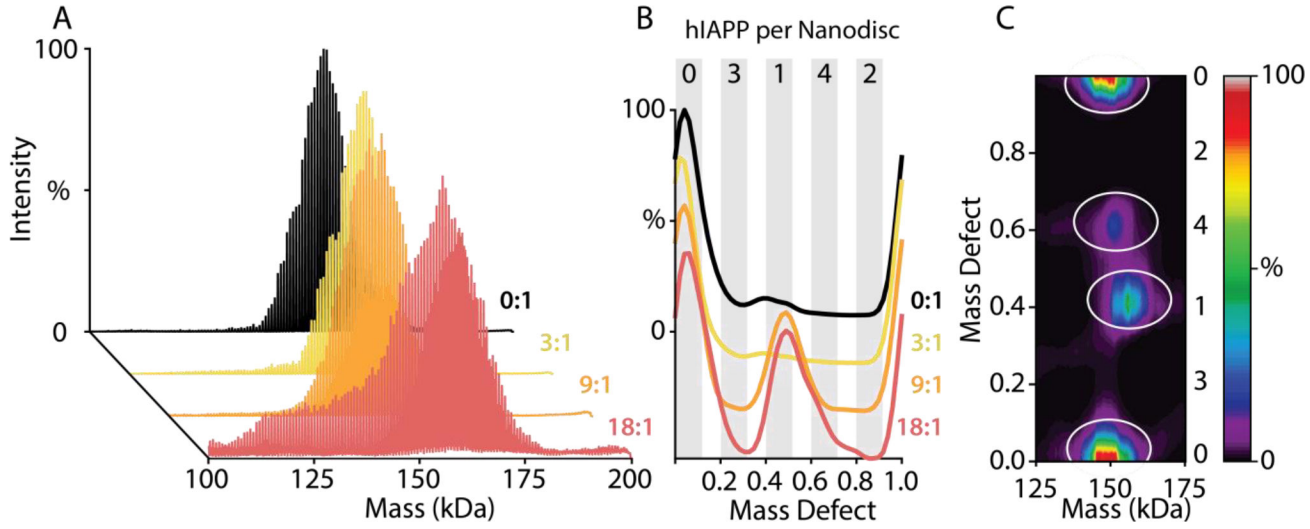

Figure 1.

Deconvolved mass spectra of (A) DPPG nanodiscs at hIAPP:nanodisc ratios of 0:1 (*black*), 3:1 (*yellow*), 9:1 (*orange*), and 18:1 (*red*) after incubation for 30 min at room temperature. (B) The mass defects at increasing hIAPP:nanodisc ratios are shown to track concentration dependent hIAPP–membrane associations. (C) A heatmap for 18:1 hIAPP:nanodisc reveals complexes with 0, 1, and 4 hIAPP per nanodisc. The predicted mass defect values (Table S1) for different hIAPP stoichiometries per nanodisc are annotated with grey bars in 1B and numbered alongside the plot in 1C.

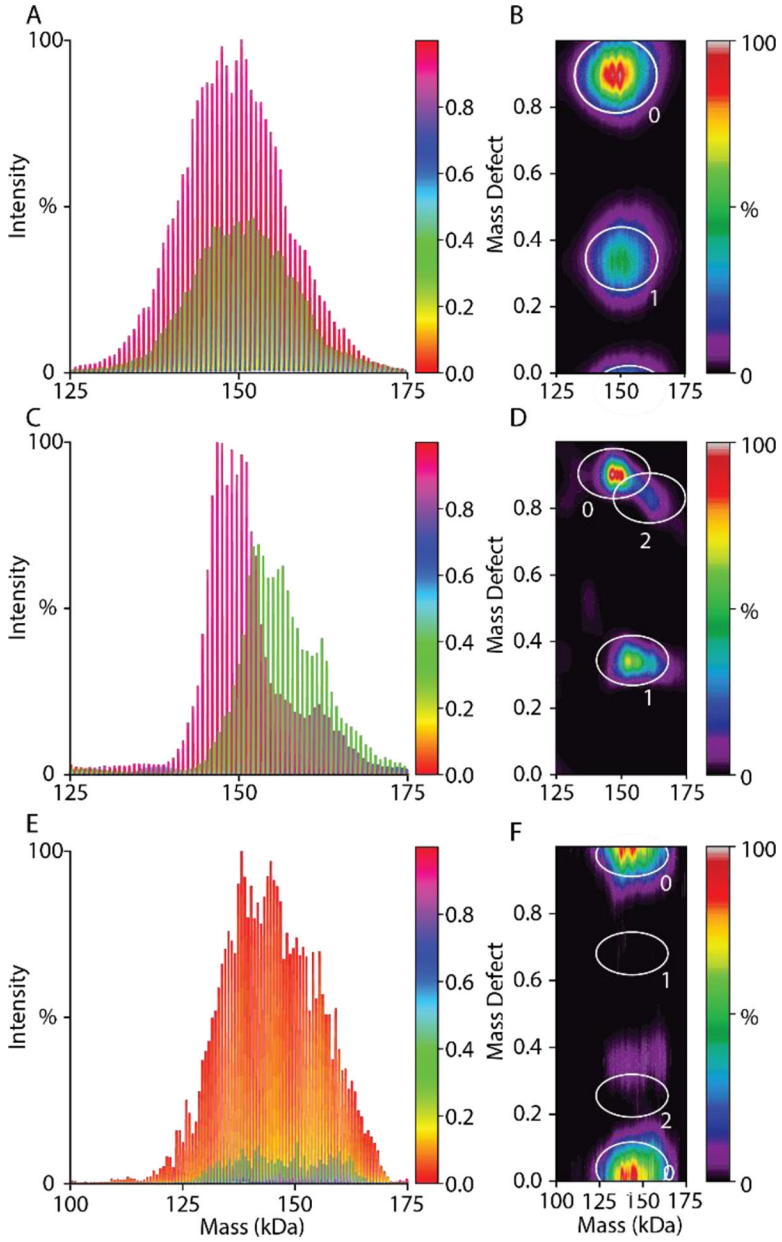

Figure 2.

Deconvolved mass spectra (A, C, E) and mass defect analysis (B, D, E) of DPPG nanodiscs at 9:1 IAPP:nanodisc ratios with (A, B) hIAPP, (C, D) rIAPP and (E, F) pIAPP. The predicted mass defect values (Table S1) for different IAPP stoichiometries per nanodisc are annotated with white circles in B, D, and F.